Study of the doubly radiative decay $J/\psi \to \gamma\gamma\rho^0$

D. Coffman, F. DeJongh, G. Dubois, G. Eigen, J. Hauser, D. G. Hitlin,
C. G. Matthews, A. Mincer, J. D. Richman, W. J. Wisniewski, and Y. Zhu
California Institute of Technology, Pasadena, California 91125

M. Burchell, D. E. Dorfan, J. Drinkard, C. Gatto, R. P. Hamilton, C. A. Heusch,
L. Köpke, W. S. Lockman, R. Partridge, H. F. W. Sadrozinski, M. Scarlatella,
T. L. Schalk, A. Seiden, A. J. Weinstein, S. Weseler, and R. Xu
University of California at Santa Cruz, Santa Cruz, California 95064

J. J. Becker, G. T. Blaylock, B. I. Eisenstein, T. Freese, G. Gladding, J. M. Izen,
S. A. Plaetzer, C. Simopoulos, A. L. Spadafora, I. E. Stockdale, and B. Tripsas
University of Illinois at Urbana-Champaign, Urbana, Illinois 61801

U. Mallik, M. Roco, and M. Z. Wang
University of Iowa, Iowa City, Iowa 52242

J. Adler, T. Bolton, J. C. Brient, K. O. Bunnell, R. E. Cassell, D. H. Coward,
K. F. Einsweiler, C. Grab, P. C. Kim, J. Labs, A. Odian, D. Pitman,
R. H. Schindler, W. Stockhausen, W. Toki, F. Villa, and S. Wasserbaech
Stanford Linear Accelerator Center, Stanford University, Stanford, California 94309

J. S. Brown, T. H. Burnett, V. Cook, A. D. Li, R. Mir, P. M. Mockett,
B. Nemati, L. Parrish, and H. J. Willutzki
University of Washington, Seattle, Washington 98195

(The Mark III Collaboration)
(Received 17 October 1989)

We present a study of the decay sequence $J/\psi \to \gamma X$, $X \to \gamma\rho^0$, $\rho^0 \to \pi^+\pi^-$, based on 5.8×10^6 produced J/ψ collected by the Mark III detector at the SLAC storage ring SPEAR. In the $\gamma\rho^0$ mass spectrum, we find two peaks with masses and widths consistent with the axial-vector mesons $f_1(1285)$ and $f_1(1420)$ that have recently been observed in two-photon collisions. Fits to the angular distributions confirm that the first peak is an axial-vector state, but are unable to distinguish between the $f_1(1420)$ or the pseudoscalar $\eta(1430)$ for the high-mass peak. Product branching fractions for both objects are presented.

I. INTRODUCTION

The $\eta(1430)$, originally known as the E and more recently as the $\iota(1440)$, attracted considerable attention as a possible glueball when it was found to be the largest noncharmonium radiative decay of the J/ψ. However, there is as yet no consensus on its quark or glue content, in part due to uncertainties about its basic properties.[1] It has been seen decaying to $K\bar{K}\pi$ and $\eta\pi\pi$ final states when it is produced hadronically, but no measurement of branching fractions to these states exists since no hadronic experiment has measured both. From J/ψ decays, the $K\bar{K}\pi$ channel appears to be dominant over the $\eta\pi\pi$ channel. The $\eta\pi\pi$ channel, however, shows a peak at lower mass, 1390 MeV, that does not appear to correspond to the $\eta(1430)$ peak in $K\bar{K}\pi$. Moreover, the peak in the $K\bar{K}\pi$ mass distribution has a higher mass, 1452 MeV, than the average for the hadronic production experiments, 1422 MeV. Lipkin[2] suggested that there are two

pseudoscalar states in this mass range, which can account for the mass spectra appearing differently depending on the mode of production. Indeed, a Dalitz-plot analysis[3] of the Mark III data on $J/\psi \to \gamma K\bar{K}\pi$ indicates that there may be three components in the $K\bar{K}\pi$ peak: The high-mass portion is predominantly pseudoscalar $K\bar{K}^*(892)$ while the lower-mass portion contains some S wave, or axial-vector $K\bar{K}^*(892)$ but mostly $a_0(980)\pi$. A more complete isobar analysis will be published soon.

There is evidence for an object in the 1.4-GeV mass region in $J/\psi \to \gamma X$, $X \to \gamma\rho^0$, in results from Mark III (Ref. 4) and two other experiments.[5] However, for all three analyses, the apparent width of the observed object is significantly larger, and the mass lower, than that of the $\eta(1430)$ seen in $K\bar{K}\pi$. Moreover, spin-parity analyses of this final state have not been performed. One must consider the possibility of contributions from the axial-vector mesons $f_1(1285)$ and $f_1(1420)$. Since these states have been seen in two-photon collisions[6] and the

$J/\psi \rightarrow \gamma f_1(1285)$ decay has been observed, one would expect contributions to $J/\psi \rightarrow \gamma\gamma\rho^0$ from these states by vector-dominance considerations. It is important to realize that since the $\gamma\gamma\rho^0$ final state represents a *double* radiative decay, the nonradiative decay modes of any objects seen must be present in J/ψ single radiative decays at much higher rates.

A study of $\eta(1430) \rightarrow \gamma\rho^0$ has been suggested[7] as important for understanding the nature of the $\eta(1430)$. Thus, we present a new analysis, with increased statistics, of the $\gamma\gamma\rho^0$ final state.

II. DATA SELECTION

The present analysis used the full 5.8×10^6 produced J/ψ Mark III data set. The Mark III detector at the SLAC storage ring SPEAR (Ref. 8) is a solenoidal magnetic spectrometer containing an inner drift chamber with 84% acceptance of charged particles surrounded by a lead-gas shower counter with 94% acceptance for photons. Events with two charged tracks and at least two photon candidates were selected. Because of the possibility of pion interactions in the shower counter, we ignore showers within 18° of the entrance of a charged particle into the shower counter, and we allow for additional showers anywhere in the detector. The shower with the highest energy is assumed to be the photon from the J/ψ radiative decay. Four-constraint (4C) fits are performed using it and one of the next two highest-energy showers to select the second photon and reject most background. The photons used in the fit are referred to as γ_{high} and γ_{low}, respectively. Events with a fit probability greater than 5% and with no more than 50 MeV total energy in candidate photons not used in the fit are selected for further analysis.

Next, a kinematic requirement is made, that $\cos\theta_1 < 0.8$, where θ_1 is the angle of the $\pi\pi$ system with respect to the γ_{high} direction in the $\pi\pi\gamma_{low}$ frame. This removes contributions from two prominent J/ψ decay
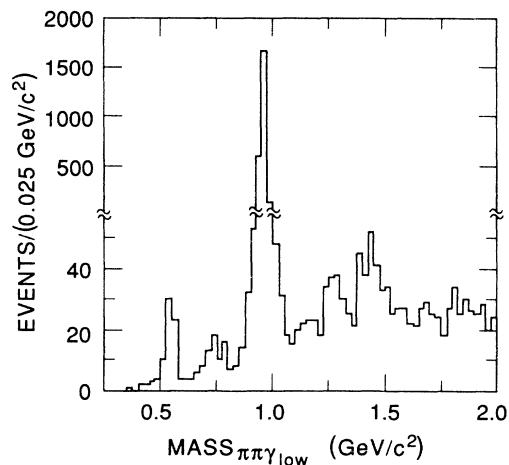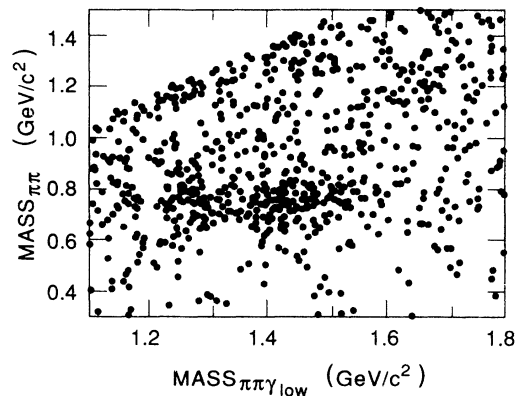
FIG. 2. Scatter plot of the $\pi\pi$ mass versus $\pi\pi\gamma_{low}$ mass.

modes: $J/\psi \rightarrow \pi^0\rho^0$ and $J/\psi \rightarrow \omega f_2$, $\omega \rightarrow \gamma\pi^0$, $f_2 \rightarrow \pi^+\pi^-$, with the π^0 decaying asymmetrically so one of its photons is not detected. The distribution of $M(\pi\pi\gamma_{low})$ is shown for the remaining events in Fig. 1.

The event sample shown in Fig. 1 is dominated by the η'. Two peaks appear at lower masses: events due to the $\pi\pi\gamma$ decay for the η, and a few events from $J/\psi \rightarrow \pi^0\rho^0$, in which the π^0 decayed asymmetrically so that one of its photons was not detected and was replaced by a "fake" photon from a pion interaction. We turn now to the two peaks with masses greater than the η' mass.

A scatter plot of $M(\pi\pi\gamma_{low})$ versus $M(\pi\pi)$, Fig. 2, indicates that the $\pi^+\pi^-$ system forms a ρ^0 for both peaks. Thus, we make a final requirement to reduce non-ρ^0 backgrounds, $0.6 < M(\pi\pi) < 0.9$ GeV. The resulting distribution in $M(\pi\pi\gamma_{low})$ is shown in Fig. 3, along with the fit described below.

III. ANALYSIS

To determine the resonance parameters we perform an unbinned maximum-likelihood fit to the data shown in
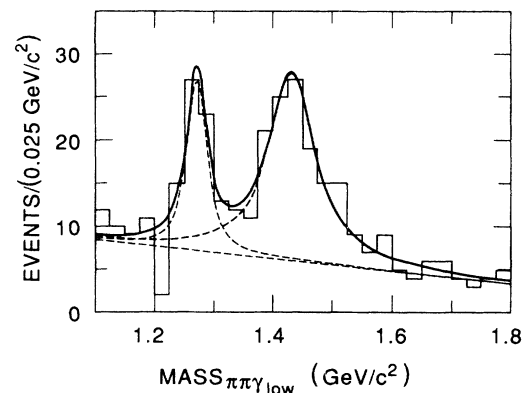
FIG. 1. Distribution of $M(\pi\pi\gamma_{low})$ for the initial data sample.

FIG. 3. Histogram of the $\pi\pi\gamma_{low}$ mass with a ρ^0 requirement, $0.6 < M_{\pi\pi} < 0.9$ GeV. The curves are a fit to the data contained in the plot.

TABLE I. Fits to the $\pi\pi\gamma_{\text{low}}$ mass distribution and comparisons with known states.

	Mass (MeV)	Width (MeV)	Events
	D region		
Fit	1271±7	31±14	45±13
$\eta(1280)$	1279±5	32±10	
$f_1(1285)$	1283±5	25±3	
	E region		
Fit	1432±8	90±26	117±22
$\eta(1430)$	1440±20	60±30	
$f_1(1420)$	1422±10	55±3	

Fig. 3. The fit function, which is overplotted on Fig. 3, consists of a linear background plus the incoherent sum of two relativistic Breit-Wigner resonances folded with the Gaussian mass resolution of 9 MeV. The parameters of the fit are shown in Table I, along with statistical errors. We defer calculation of the corresponding branching fractions until a discussion of the angular fits. We refer to the mass ranges containing the peaks 1.20–1.35 GeV and 1.35–1.50 GeV as *D* and *E*, respectively. For comparison, Table I also shows the Particle Data Group[1] (PDG) values for the pseudoscalar $\eta(1280)$ and $\eta(1430)$, as well as the axial vector $f_1(1285)$ and $f_1(1420)$.

Since a fit to the mass distribution cannot uniquely identify either peak, we have also performed an angular analysis. The sequence of three reactions $e^+e^- \rightarrow \gamma X$, $X \rightarrow \gamma\rho^0$, $\rho^0 \rightarrow \pi^+\pi^-$ is characterized by five angles: θ_γ, the angle of the first photon with respect to the e^+ direction; θ_1 and ϕ_1, the angles of the ρ^0 in the helicity frame of X; and θ_2 and ϕ_2, the angles of the π^+ in the ρ^0 helicity frame.[9]

We test the hypotheses that each peak is predominantly pseudoscalar or axial vector by fitting the angular distributions of the events in the two regions to either 0^- or 1^+ plus a phase-space background. The signal fractions in the fit are set to values determined by the mass fit, 53% and 66% for the *D* and *E* regions, respectively. Allowing the signal fraction to vary does not significantly alter the results. There are no free parameters for 0^-. For the 1^+ hypothesis, the production reaction $J/\psi \rightarrow \gamma X$ is described by two helicity amplitudes A_0 and $A_1 = A_{-1}$; there are also two helicity amplitudes describing the decay reaction $X \rightarrow \gamma\rho^0$, B_0 and $B_1 = B_{-1}$. We determine the product $A_0 B_1$ by the number of events. This leaves the two complex ratios, A_1/A_0 and B_0/B_1, as parameters. Since the imaginary parts of the ratios were consistent with zero, we fixed them at zero for the
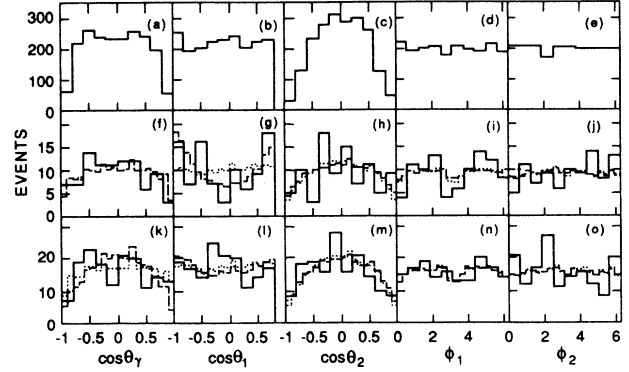

FIG. 4. Angular distributions for the η' [(a)–(e)], the *D* region [(f)–(j)] and the *E* region [(k)–(o)]. In plots [(f)–(o)], the dotted and dashed lines represent fits to phase space plus 0^- and 1^+, respectively. Note that the fits to 0^- and 1^+ are nearly coincident in all the plots except for (g).

fits presented in Table II. Examining the likelihood ratio of the two candidate hypotheses in each mass region, we find in the *D* region that the 1^+ hypothesis is preferred over 0^- by a likelihood ratio of 2200, or $\sim 4\sigma$, while the *E* region fits 0^- slightly better than 1^+ by a likelihood ratio of 9.0, or $\sim 2\sigma$.

Figure 4 contains plots of the five angles for the *D* and *E* mass regions, and the η' for comparison. The *D* and *E* region distributions are overplotted with the fit 0^- and 1^+ distributions (dotted and dashed, respectively) as predicted by the Monte Carlo acceptance. Examining Fig. 4(g), of $\cos\theta_1$, it is apparent why the 1^+ is preferred for the *D* region. This distribution should be flat for phase space or 0^-. The apparent $\cos^2\theta_1$ behavior corresponds to both helicity ratios being zero; that is, longitudinal production of the 1^+ state and its subsequent decay to a transversely polarized ρ^0. In this case, the distribution is $(1+\cos^2\theta_\gamma)\cos^2\theta_1\sin^2\theta_2$, which differs from the corresponding 0^- distribution by the factor $\cos^2\theta_1$.

Careful consideration[4] has been given to potential background processes. Particle identification, when available, confirms that the charged tracks are pions. Other decays producing the final state $\gamma\gamma\pi^+\pi^-$ (e.g., $\rho^0\pi$) have been examined and do not contribute to the signal observed. It is possible for a final state with more than two photons to "feed down" if the photons are unobserved or have small enough energies. However, C invariance requires that there must be an even number of additional photons. Thus, there must be at least two real photons not used in the kinematic fit for such a process to fake our signal. This possibility is eliminated by exam-

TABLE II. Angular-fit results.

Mass range (GeV)	Events	Signal fraction	Log likelihood $0^- - 1^+$	Helicity ratios for 1^+	
				A_1/A_0	B_0/B_1
1.2–1.35	92	53%	−7.7	0.35±0.19	−0.33±0.16
1.35–1.5	118	66%	2.2	−1.0±0.2	0.31±0.15

ination of the kinematic fit probability distribution, which has a uniformly distributed component consistent with the signal, and by explicit study of final states such as $\rho^0\pi^0\pi^0$.

The Monte Carlo event sample that was used to calculate normalizations for the angular analysis described above was also used to determine the detection efficiency. However, the requirements on the kinematic fit probabili-

ty and extra shower energy are not well modeled by the simulation. We estimate these efficiencies instead by a study of the effects of these requirements on the η' events. The resulting net efficiency is $(31.5\pm1.4)\%$. The systematic error in the following is determined by adding the error in the efficiency in quadrature with the 8.5% uncertainty in the number of produced J/ψ. Thus, we obtain

$$B(J/\psi \to \gamma f_1(1285))B(f_1(1285) \to \gamma\rho^0) = (0.25\pm0.07\pm0.03)\times10^{-4},$$

$$B(J/\psi \to \gamma X(1432))B(X(1432) \to \gamma\rho^0) = (0.64\pm0.12\pm0.07)\times10^{-4}.$$

IV. DISCUSSION

Our study of the double radiative decay $J/\psi \to \gamma\gamma\rho^0$ has resolved the broad peak seen previously in this channel into two peaks. The lower-mass peak is unambiguously identified as due to the axial-vector meson $f_1(1285)$ but the $X(1432)$ is not distinguishable between the pseudoscalar $\eta(1430)$, the axial-vector $f_1(1420)$, or indeed a mixture of the two.

The angular analysis that identified the lower-mass peak indicates that it is produced primarily with longitudinal polarization, and decays into a transversely polarized ρ^0. Combining the above product branching fraction with the Mark III measurement[10] of the product branching fraction for $J/\psi \to \gamma f_1(1285) \to \gamma 4\pi$, the PDG values for $B(f_1(1285) \to 4\pi)$ and the total width, we obtain $\Gamma(f_1(1285) \to \gamma\rho^0) = 1.7\pm0.7$ MeV.

The decay polarization of the ρ^0 in the $f_1(1285)$ decay was predicted to be transverse by Babcock and Rosner[11] based on vector-meson dominance and the quark transition hypothesis. However, they predict a partial width of ~ 140 keV, a factor of 12 smaller than our observation. The production mechanism for noncharmonium J/ψ decays is expected to be dominated by two intermediate gluons. Cahn[12] has studied the similar production reaction $\gamma\gamma^* \to f_1$ to explain the two-photon results discussed earlier. He predicts that the f_1 is produced with

primarily longitudinal polarization, as observed here. Finally, a perturbative QCD calculation[13] predicts $B(J/\psi \to \gamma f_1(1285)) = 10^{-3}$, about a factor of 4 larger than observed, with the f_1 produced mostly longitudinally.

We turn to the $X(1432)$. The fact that the $\gamma\gamma\rho^0$ final state represents two radiative decays implies that the singly radiative process also be present in J/ψ decays at a much larger rate. Of the possible hadronic final states to which an axial-vector or pseudoscalar object could decay, $\eta\pi\pi$, 4π, and $K\bar{K}\pi$, only $K\bar{K}\pi$ has a corresponding peak, the $\eta(1430)$. If we identify $X(1432)$ with the $\eta(1430)$, then we infer a ratio of branching fractions for the $\eta(1430)$: $B(\eta(1430) \to \gamma\rho^0)/B(\eta(1430) \to K\bar{K}\pi) = (1.4\pm0.4)\times10^{-2}$. One should keep in mind, however, the evidence quoted in the Introduction that the $K\bar{K}\pi$ object is compound, which could mean that the $X(1432)$ represents a different mixture.

ACKNOWLEDGMENTS

[1]Particle Data Group, G. P. Yost et al., Phys. Lett. B 204, 1 (1988). See p. 294 for a review.

[2]H. J. Lipkin, Phys. Lett. B 171, 298 (1986).

[3]T. H. Burnett, in Glueballs, Hybrids and Exotic Hadrons, Upton, New York, 1988, edited by S-U. Chung (AIP Conf. Proc. No. 185) (AIP, New York, 1989).

[4]J. Richman, in QCD and Beyond, proceedings of the XXth Rencontre de Moriond, Les Arcs, France, 1985, edited by J. Tran Thanh Van (Editions Frontieres, Gif-sur-Yvette, 1985); Ph.D. thesis, CALT-68-1231, 1985.

[5]C. Edwards, Ph.D. thesis, California Institute of Technology Report No. CALT-68-1165, 1985; J. E. Augustin et al., Orsay Report No. LAL/85-27, 1985 (unpublished).

[6]A. Aihara et al., Phys. Rev. Lett. 57, 2500 (1986); G. Gidal et al., Phys. Rev. Lett. 59, 2012 (1987); 59, 2016 (1987).

[7]M. Chanowitz, Phys. Lett. 164B, 379 (1985); Milton Dean Slaughter and S. Oneda, Phys. Rev. Lett. 59, 1641 (1987).

[8]D. Bernstein et al., Nucl. Instrum. Methods A226, 301 (1984).

[9]Note that with our definition, ϕ_1 is the difference between the azimuthal angles of the e^+ and ρ^0, about the X direction.

[10]R. Mir, in Proceedings of the VIIIth International Workshop on Photon-Photon Collisions, Shoresh, Israel, 1988, edited by U. Karshan (World Scientific, Singapore, 1988).

[11]J. Babcock and J. L. Rosner, Phys. Rev. D 14, 1286 (1976); J. L. Rosner, ibid. 23, 1127 (1981).

[12]R. N. Cahn, Phys. Rev. D 35, 3342 (1987); 37, 833 (1988).

[13]J. G. Körner, J. H. Kühn, M. Krammer, and H. Schneider, Nucl. Phys. B229, 115 (1983).